Monitoring Surface Reactions at an AFM Tip: An Approach To Follow Reaction Kinetics in Self-Assembled Monolayers on the Nanometer Scale

Holger Schönherr,[†] Victor Chechik,[‡,§] Charles J. M. Stirling,*[,‡] and G. Julius Vancso*[,†]

Contribution from the MESA[+] Research Institute and Faculty of Chemical Technology, Materials Science and Technology of Polymers, University of Twente, P.O. Box 217, 7500 AE Enschede, The Netherlands, and Department of Chemistry and Centre for Molecular Materials, University of Sheffield, Sheffield S3 7HF, U.K.

Received January 25, 1999. Revised Manuscript Received October 15, 1999

Abstract: The kinetics of alkaline hydrolysis of ester groups in self-assembled monolayers (SAMs) were monitored by a combination of atomic force microscopy (AFM) on the nanometer scale and FT-IR spectroscopy in the continuum limit. The main objective was to study surface reactions in situ with chemical specificity, from the nanometer perspective, using an atomic force microscope. This could not be achieved by conventional AFM friction or force measurements due to insufficient resolution, and instrumental or thermal drift, respectively. These problems were circumvented by a novel approach, which we termed "inverted" chemical force microscopy (ICFM). In ICFM, chemical reactions, which take place at the surface of the tip coated with reactants, are probed in situ by force−distance measurements on a scale of less than 100 molecules. The pull-off forces of different reactive SAMs were shown to vary with the extent of the reaction. Reactivity differences for these monolayers observed in this manner by AFM on the nanometer scale agree well with macroscopic behavior observed by FT-IR and can be related to differences in the SAM structure. These results, together with additional force microscopy data, support the conclusion that, for closely packed ester groups, the reaction spreads from defect sites, causing separation of the homogeneous surfaces into domains of reacted and unreacted molecules.

Introduction

Self-assembled monolayers (SAMs) of organic molecules on solid substrates are becoming increasingly important for various technologies. Areas of possible application range from surface modifications for wettability control,[1] tribology, or lubrication[2] to sensors,[3] devices, or surface patterning (soft lithography).[4] Beyond their practical importance, SAMs offer unique opportunities to enhance our fundamental understanding of interfacial phenomena.[1] They can serve as well-defined model systems to study the behavior of surfaces at the ultimate limit of atomic detail. Although surface science techniques are generally developing rapidly and allow one to characterize surfaces with improving lateral spatial resolution,[5] in situ molecular-level studies of *chemical reactions* have largely eluded surface scientists until recently. Therefore, if one wants to obtain a better understanding of these processes at the level of single molecules, novel approaches must be developed to examine chemical reactions occurring at surfaces and interfaces.

When functional groups are confined in closely packed molecular arrays, their reactivity often changes. For example, Töllner et al. reported significantly enhanced catalysis of acetone hydrogenation probably because of enforced (favorable) orientation of a rhodium complex incorporated in corresponding Langmuir−Blodgett films.[6] Penetration of external reagents to functional groups buried in a well-packed monolayer is usually restricted, and reactivity is thus reduced. We have shown earlier that monolayers of aliphatic esters with the carboxyl group buried 10 methylene groups below the surface show a remarkable stability toward transesterification.[7] Well-packed monolayers of isonicotinate esters were shown to hydrolyze only very

* Authors to whom correspondence should be addressed.
† University of Twente.
‡ University of Sheffield.
§ Present address: Department of Chemistry, University of York, Heslington, York YO10 5DD, U.K.

(1) (a) Ulman, A. *An Introduction to Ultrathin Organic Films: From Langmuir−Blodgett to Self-Assembly*; Academic Press: New York, 1991. (b) Bishop, A. R.; Nuzzo, R. G. *Curr. Opin. Colloid Interface Sci.* **1996**, *1*, 127−136. (c) Dubois, L. H.; Nuzzo, R. G. *Annu. Rev. Phys. Chem.* **1992**, *43*, 437−463.

(2) (a) Carpick, R. W.; Salmeron, M. *Chem. Rev.* **1997**, *97*, 1163−1194. (b) Lio, A.; Charych, D. H.; Salmeron, M. *J. Phys. Chem. B* **1997**, *101*, 3800−3805.

(3) (a) Rubinstein, I.; Steinberg, S.; Tor, Y.; Shanzer, A.; Sagiv, J. *Nature* **1988**, *332*, 426−429. (b) Rubinstein, I.; Steinberg, S.; Tor, Y.; Shanzer, A.; Sagiv, J. *Nature* **1989**, *337*, 217−217. (c) Turyan, I.; Mandler, D. *Anal. Chem.* **1994**, *66*, 58−63. (d) Gafni, Y.; Weizman, H.; Libman, J.; Shanzer, A.; Rubinstein, I. *Eur. J. Chem.* **1996**, *2*, 759−766. (e) Kepley, L. J.; Crooks, R. M.; Ricco, A. J. *Anal. Chem.* **1992**, *64*, 3191−3193. (f) Schierbaum, K.-D.; Weiss, T.; Thoden van Velzen, E. U.; Engbersen, J. F. J.; Reinhoudt, D. N.; Göpel, W. *Science* **1994**, *265*, 1413−1415. (g) Mrksich, M.; Grunwell, J. R.; Whitesides, G. M. *J. Am. Chem. Soc.* **1995**, *117*, 12009−12010. (h) Mrksich, M.; Sigal, G. B.; Whitesides, G. M. *Langmuir* **1995**, *11*, 4383−4385. (i) Huisman, B.-H.; Kooyman, R. P. H.; van Veggel, F. C. J. M.; Reinhoudt, D. N. *Adv. Mater.* **1996**, *8*, 561−564.

(4) (a) Kumar, A.; Abbott, N. L.; Kim, E.; Biebuyck, H. A.; Whitesides, G. M. *Acc. Chem. Res.* **1995**, *28*, 219−226. (b) Kumar, A.; Biebuyck, H. A.; Whitesides, G. M. *Langmuir* **1994**, *10*, 1498−1511. (c) Wilbur, J. L.; Kumar, A.; Kim, E.; Whitesides, G. M. *Adv. Mater.* **1994**, *6*, 600−604. (d) Kumar, A.; Whitesides, G. M. *Science* **1994**, *263*, 60−62. (e) Jackman, J. R.; Wilbur, J. L.; Whitesides, G. M. *Science* **1995**, *269*, 664−666. (f) Xia, Y.; Whitesides, G. M. *Adv. Mater.* **1995**, *7*, 471−473.

(5) *Practical Surface Analysis*; Briggs, D., Seah, M. P., Eds.; Wiley: Chichester, 1992.

(6) Töllner, K.; Popovitz-Biro, R.; Lahav, M.; Milstein, D. *Science* **1997**, *278*, 2100−2102.

(7) Neogi, P.; Neogi, S.; Stirling, C. J. M. *J. Chem. Soc., Chem. Commun.* **1993**, 1134−1135.

10.1021/ja9902569 CCC: $19.00 © 2000 American Chemical Society
Published on Web 03/30/2000

slowly.[8] Many biological reactions occur at similarly well-ordered interfaces. The course of such important reactions, however, remains largely unknown, and they could be susceptible to the procedures described here.

The recent developments in the field of scanning probe techniques promise to give novel insights into processes that occur at surfaces or interfaces. Surface studies with nominal nanometer resolution can be carried out in different media or environments. It is therefore not surprising that surface processes have been studied in the past with high-resolution scanning probe microscopies.[9] Ex situ AFM using chemically modified tips has been shown to provide information about surface energy changes related to interfacial reactions.[10] Previously, in situ AFM was primarily applied to monitor topographical changes, e.g., in crystal growth or dissolution, in crystallization of polymers from the melt, and in solid-state isomerization reactions.[11]

All the aforementioned observations are, in general, limited by the finite contact area between the AFM tip and the sample surface. Depending on the radius of curvature of the AFM tips, on the materials properties, and on the imaging force, the radius of the contact area can be estimated to be between 2 and 5 nm.[12] As a consequence, the *true* resolution is often *much* lower than the nominal accuracy of positioning the specimen and the sensitivity of height or lateral force data.[13,14] The "high" resolution obtained with conventional contact mode AFM (e.g., for periodic lattice structures found for SAMs)[15] can be considered a "lattice resolution". As shown recently,[16] lattice resolution can be considered as an average over the periodic electron density distribution of the actual contact area. In any case, the expected resolution of AFM in imaging of surfaces in liquid can be assumed to be no better than several nanometers.

In addition, thermal and instrumental drift make high-resolution imaging of chemical reactions very difficult or impossible. For instance, we observed pronounced scatter in the data obtained in a study of kinetics of inhomogeneous reactions in SAMs by conventional force−distance measurements. The scatter was attributed to the aforementioned drift which results in interactions between different areas of the SAM with the AFM tip. Since the area imaged is, in general, changing constantly, and furthermore "reference points" such as topographical features might change, as well, as a consequence of the reaction, the lateral resolution is poorer than the true physical resolution discussed above.

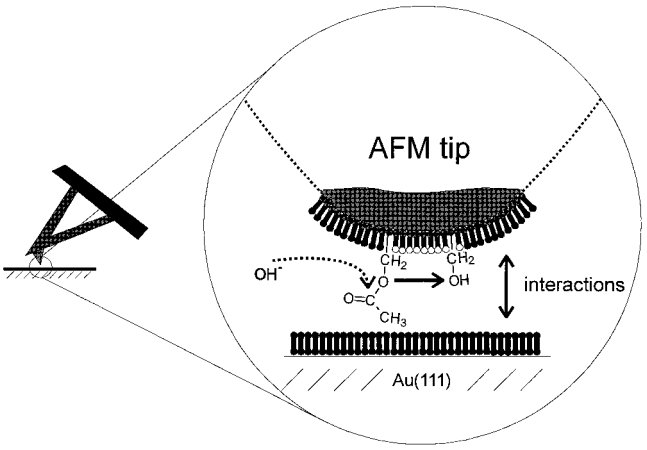

Figure 1. In "inverted" chemical force microscopy the pull-off forces of a reactant-covered AFM tip are measured in situ during the conversion of the reactive groups. The interaction between tip and inert surface varies with the extent of the reaction. The approach is depicted schematically for the reaction of ester groups to hydroxyl groups in aqueous NaOH.

In this paper, a novel approach to study surface reactions of organic thin films with nanometer-level adhesion measurements using AFM is described. In this novel approach, the reactants are immobilized on the AFM tip rather than on the sample surface (Figure 1).[17] The variation of pull-off forces[18] between the tip coated with the reactant and an inert surface is consecutively monitored as a function of time.[19] The contact area of the tip at pull-off in such experiments using nonreactive SAMs (as inert samples) deposited on Au(111) varies between approximately 10 and 100 effectively interacting molecular pairs.[20,21] In general, as has been predicted by contact mechanics

(8) van Ryswyk, H.; Turtle, E. D.; Watson-Clark, R.; Tanzer, T. A.; Herman, T. K.; Chong, P. Y.; Waller, P. J.; Taurog, A. L.; Wagner, C. E. *Langmuir* **1996**, *12*, 6143−6150.

(9) Scanning tunneling microscopy (STM) is, in general, limited to (semi)conducting samples. For a recent review, see, e.g.: Somorjai, G. A. *Chem. Rev.* **1996**, *96*, 1223−1236 and references therein. In addition, the STM tip can induce changes in the surface (Touzov, I.; Gorman, C. B. *J. Phys. Chem.* **1997**, *101*, 5263−5276). In the case of a thick layer of adsorbate, the feedback loop, which keeps a constant tunneling current during scanning, will cause the tip to penetrate into the material, resulting in high shear forces.

(10) (a) Werts, M. P. L.; van der Vegte, E. W.; Hadziioannou, G. *Langmuir* **1997**, *13*, 4939−4942. (b) Schönherr, H.; Hruska, Z.; Vancso, G. J. *Macromolecules* **1998**, *31*, 3679−3685. (c) Schönherr, H.; Vancso, G. J. *J. Polym. Sci. B, Polym. Phys.* **1998**, *36*, 2486−2492.

(11) (a) Gidalewitz, D.; Feidenhans'l, R.; Matlis, S.; Smilgies, D.-M.; Christensen, M. J.; Leiserowitz, L. *Angew. Chem., Int. Ed. Engl.* **1997**, *36*, 955−959. (b) Pearce R.; Vancso, G. J. *Macromolecules* **1997**, *30*, 5843−5848. (c) Kaupp, G.; Haak, M. *Angew. Chem., Int. Ed. Engl.* **1996**, *35*, 2774−2777. (d) Kautek, W.; Dieluweit, S.; Sahre, M. *J. Phys. Chem. B* **1997**, *101*, 2709−2715. (e) Wall, J. T.; Grieser, F.; Zukoski, C. F. *J. Chem. Soc., Faraday Trans.* **1997**, *93*, 4017−4020.

(12) The estimation is based on Hertz theory as described in ref 16. For a normal force of 2 nN and a tip radius of 5 nm, a contact radius of 1.8 nm can be estimated. However, typical radii of modified AFM tips are of the order of 50−75 nm. This leads to a radius of the contact area of 4.0−4.5 nm.

(13) True atomic resolution has been reported for experiments with custom-made force microscopes which operate under UHV conditions: (a) Giessibl, F. J. *Science* **1995**, *267*, 68−71. (b) Güthner, P. J. *Vac. Sci. Technol. B* **1996**, *14*, 2428. (c) Kitamura, S.; Iwatsuki, M. *Jpn. J. Appl. Phys.* **1995**, *34*, L145. (d) Kitamura, S.; Iwatsuki, M. *Jpn. J. Appl. Phys.* **1996**, *35*, L668. (e) Defect motion was observed on InP(110) surfaces with noncontact AFM: Sugawara, Y.; Ohta, M.; Ueyama, H.; Morita, S. *Science* **1995**, *270*, 1646.

(14) Intermittent contact modes are often used to obtain true atomic resolution; see, e.g., a report on true atomic resolution obtained by AFM on isolator surfaces: Bammerlin, M.; Lüthi, R.; Meyer, E.; Baratoff, A.; Guggisberg, M.; Gerber, Ch.; Howald, L.; Güntherodt, H.-J. *Probe Microsc.* **1997**, *1*, 3−10.

(15) SAMs were subject to numerous studies by AFM, see, e.g.: (a) Alves, C. A.; Smith, E. L.; Porter, M. D. *J. Am. Chem. Soc.* **1992**, *114*, 1222−1227. (b) Pan, J.; Tao, N.; Lindsay, S. M. *Langmuir* **1993**, *9*, 1556−1560. (c) Alves, C. A.; Porter, M. D. *Langmuir* **1993**, *9*, 3507−3512. (d) Butt, H.-J.; Seifert, K.; Bamberg, E. *J. Phys. Chem.* **1993**, *97*, 7316−7320. (e) Liu, G.-Y.; Salmeron, M. *Langmuir* **1994**, *10*, 367. (f) Liu, G.-Y.; Fenter, P.; Chidsey, C. E. D.; Ogletree, D. F.; Eisenberger, P.; Salmeron, M. *J. Chem. Phys.* **1994**, *101*, 4301−4306. (g) Wolf, H.; Ringsdorf, H.; Delamarche, E.; Takami, T.; Kang, H.; Michel, B.; Gerber, Ch.; Jaschke, M.; Butt, H.-J.; Bamberg, E. *J. Phys. Chem.* **1995**, *99*, 7102−7107. (h) Jaschke, M.; Schönherr, H.; Wolf, H.; Butt, H.-J.; Bamberg, E.; Besocke, M. K.; Ringsdorf, H. *J. Phys. Chem.* **1996**, *100*, 2290−2301. (i) Schönherr, H.; Vancso, G. J.; Huisman, B.-H.; van Veggel, F. C. J. M.; Reinhoudt, D. N. *Langmuir* **1997**, *13*, 1567−1570.

(16) (a) Nelles, G.; Schönherr, H.; Vancso, G. J.; Butt, H.-J. *Appl. Phys. A* **1998,** *66*, S1261 − S1266. (b) Nelles, G.; Schönherr, H.; Jaschke, M.; Wolf, H.; Schaub, M.; Küther, J.; Tremel, W.; Bamberg, E.; Ringsdorf, H.; Butt, H.-J. *Langmuir* **1998**, *14*, 808−815.

(17) The use of chemically functionalized probe tips in AFM is known in the literature as "chemical force microscopy". The group of Lieber showed that the terminal functional groups of SAMs of ω-functionalized thiols on gold-coated AFM tips can dominate the adhesive or frictional interactions with the surface (Frisbie, C. D.; Rozsnyai, L. F.; Noy, A.; Wrighton, M. S.; Lieber, C. M. *Science* **1994**, *265*, 2071−2074).

(18) Weisenhorn, A. L.; Maivald, P.; Butt, H.-J.; Hansma, P. K. *Phys. Rev. B* **1992**, *45*, 11226−11232.

Chart 1. Compounds Used To Prepare Self-Assembled Monolayers

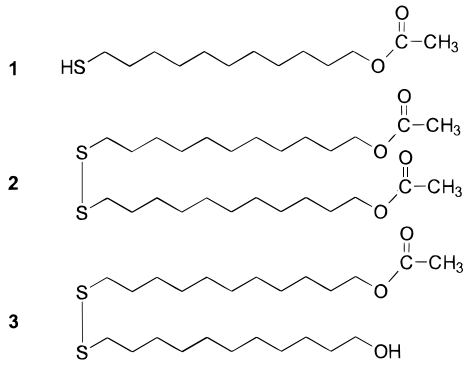

theories, the contact area at pull-off is smaller than the contact area during scanning.[22] Thus, pull-off force measurements are anticipated to have higher resolution.

Depending on the changes in the pull-off forces with the extent of the reaction, the effective force per interacting molecular pair, as well as the number of interacting pairs, can vary.[23] Thus, one can, in principle, monitor chemical reactions with a resolution of the number of contacting molecular pairs in AFM force measurements, provided that the conversion of the reactants to products is accompanied by changes in the pull-off forces. The force contrast can be controlled since the magnitude of the pull-off force depends on the choice of the inert substrate.[24] Thus, a large variety of different systems can, in principle, be studied. As demonstrated here, the kinetics of surface reactions can be followed in situ on a *noncontinuum* level (10−100 molecules) by this technique, which we termed "inverted" chemical force microscopy.

In the current paper, "inverted" chemical force microscopy and FT-IR spectroscopy were applied to study the kinetics of alkaline hydrolysis of ester groups at the surface of self-assembled monolayers. The results of kinetic measurements averaged over a large area (by FT-IR),[25] nanometer-scale kinetic information (by inverted CFM), and additional high-resolution force microscopy allowed us to elucidate the reaction mechanism. For closely packed ester groups, the reaction was concluded to spread from defect sites, causing separation of the homogeneous surfaces into domains of reacted and unreacted molecules.

Table 1. SAM Characteristics

	contact angles (water), deg			
compound	advancing	sessile	receding	SPR thickness, Å
1	70	68	64	11
2	66	62	56	11
3	57	52	44	12

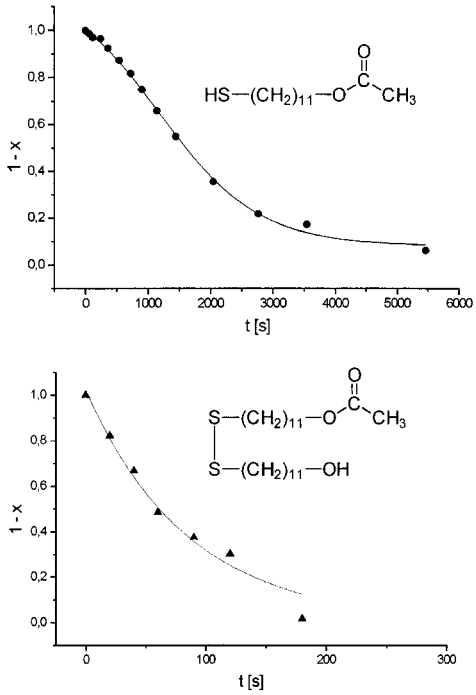

Figure 2. Reaction kinetics in the continuum limit for the hydrolysis in 1 M NaOH as determined by FT-IR for thiol **1** (top) and disulfide **3** (bottom).

Experimental Section

Materials. HPLC-grade dichloromethane and ethanol were purchased from Aldrich and used as such. Millipore Milli-Q water was used in all experiments. 11-Mercaptoundecyl acetate **1** was synthesized as described earlier.[26]

Disulfides 2 and 3. Acetyl chloride (0.65 mmol) in ethyl acetate was added to the solution of bis(11-hydroxyundecyl) disulfide[26] (0.43 mmol) in dry ethyl acetate (10 mL) at 30 °C. The mixture was stirred at 50 °C for 4 h, and solvent was evaporated. Crude product was purified by flash chromatography from ether:CH_2Cl_2 1:6. The first-eluted compound (R_f 0.8) was further chromatographed from ether:petroleum ether 1:4 (R_f 0.25) to give 50 mg of disulfide **2**, mp 31−32 °C. IR (cast film), cm^{-1}: $\nu(CH_2)$ 2919, 2850, $\nu(C{=}O)$ 1732, $\delta_{sc}(CH_2)$ 1471, $\delta_s(CH_3)$ 1370, $\nu(C{-}O)$ 1242, 1049. ^1H NMR ($CDCl_3$): δ 4.04 (t, 4H, CH_2O), 2.66 (t, 4H, CH_2S), 2.03 (s, 6H, CH_3), 1.2−1.7 (m, 36H, $CH_2CH_2CH_2$). Anal. Calcd for $C_{26}H_{50}O_4S_2$: C, 63.63; H, 10.27. Found: C, 63.34; H, 10.46.

The second-eluted compound (R_f 0.37) was mixed disulfide **3**, yield 80 mg, mp 53.5−54 °C. IR (cast film), cm^{-1}: ν(OH) 3363, $\nu(CH_2)$ 2919, 2850, $\nu(C{=}O)$ 1731, $\delta_{sc}(CH_2)$ 1470, $\delta_s(CH_3)$ 1368, $\nu(C{-}O)$ 1241,

(19) Compared to pull-off force measurements on Au(111) substrates modified with reactants, this procedure eliminates the problem of thermal and instrumental drift which results in lateral displacement of the sampling area (contact area at pull-off). Thus, the adhesion between the *same* molecules (functional groups) and the homogeneous inert substrate are measured.

(20) (a) Noy, A.; Frisbie, C. D.; Rozsnyai, L. F.; Wrighton, M. S.; Lieber, C. M. *J. Am. Chem. Soc.* **1995**, *117*, 7943−7951. (b) Vezenov, D. V.; Noy, A.; Rozsnyai, L. F.; Lieber, C. M. *J. Am. Chem. Soc.* **1997**, *119*, 2006−2015. (c) Noy, A.; Vezenov, D. V.; Lieber, C. M. *Annu. Rev. Mater. Sci.* **1997**, *27*, 381−421.

(21) In recent reports on functionalized carbon nanotubes as tip apexes, it was demonstrated that smaller tip radii and thus contact areas are, in principle, accessible ((a) Wong, S. S.; Joselevich, E.; Woolley, A. T.; Cheung, C. L.; Lieber, C. M. *Nature* **1998**, *394*, 52−55. (b) Wong, S. S.; Woolley, A. T.; Joselevich, E.; Cheung, C. L.; Lieber, C. M. *J. Am. Chem. Soc*. **1998**, *120*, 8557−8558.). The tip chemistry, degree of functionalization, and lateral confinement of reactive groups are, however, better controlled using self-assembled monolayers.

(22) Israelachvili, J. N. *Intermolecular and Surface Force*s, 2nd ed.; Academic Press: London, 1991; p 326.

(23) (a) Thomas, R. C.; Tangyunyong, P.; Michalske, T. A.; Crooks, R. M. *J. Phys. Chem.* **1994**, *98*, 4493−4494. (b) Green, J.-B. D.; McDermott, M. T.; Porter, M. D.; Siperko, L. M. *J. Phys. Chem.* **1995**, *99*, 10960−10965. (c) Akari, S.; Horn, D.; Keller, H.; Schrepp, W. *Adv. Mater*. **1995**, *7*, 549−551. (d) Sinniah, S. K.; Steel, A. B.; Miller, C. J.; Reutt-Robey, J. E. *J. Am. Chem. Soc.* **1996**, *118*, 8925−8931. (e) Schönherr, H.; Vancso, G. J. *Macromolecules* **1997**, *30*, 6391−6394. (f) van der Vegte, E. W.; Hadziioannou, G. *Langmuir* **1997**, *13*, 4357−4368. (g) McKendry, R.; Theoclitou, M. E.; Rayment, T.; Abbell, C. *Nature* **1998**, *391*, 566−568.

(24) Since the original report on CFM, numerous articles have been published that essentially follow along these lines of thought (see refs 20, 23). As a consequence, a large number of functional group interactions in different media is known, and thus a tip functionality can be chosen accordingly to yield high "contrast".

(25) Duevel, R. V.; Corn, R. M. *Anal. Chem*. **1992**, *64*, 337−342.

(26) Zong, K.; Brittain, S. T.; Wurm, D. B.; Kim, Y.-T. *Synth. Commun.* **1997**, *27*, 157−162.

Table 2. Half-Reaction Times $\tau_{1/2}$ As Determined by FT-IR (ex Situ Hydrolysis in 1.0 M NaOH)

SAM	$\tau_{1/2}$, s
1	1644
2	684
3	72

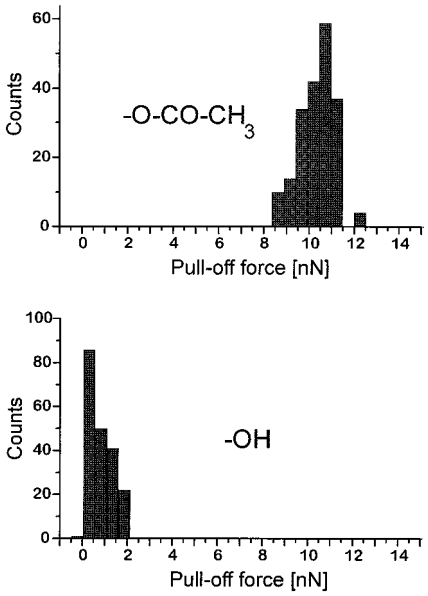

Figure 3. Histograms of pull-off forces measured with a single octadecanethiol-functionalized tip on neat SAMs of thiol **1** and 11-mercaptoundecanol in water.

1049. ^{1}H NMR ($CDCl_3$): δ 4.04 (t, 2H, CH_2OCO), 3.63 (t, 2H, CH_2-OH), 2.66 (t, 4H, CH_2S), 2.03 (s, 3H, CH_3), 1.2−1.7 (m, 36H, CH_2CH_2-CH_2). Anal. Calcd for $C_{24}H_{47}O_3S_2$: C, 64.38; H, 10.58. Found: C, 64.16; H, 10.85.

Preparation of SAMs. SAMs for FT-IR analysis were self-assembled onto evaporated gold as described in ref 27. Briefly, gold substrates were prepared by thermal evaporation of 5 nm of Cr followed by 100 nm of Au onto silicon wafers which were precleaned by heating in piranha solution (7:3 mixture of concentrated sulfuric acid and 30% hydrogen peroxide) at 90 °C for 1 h. [***Caution!*** Piranha solution reacts violently with almost any organic material and should be handled with utmost care!] Prior to deposition of monolayers, the gold substrates were treated with concentrated HNO_3 for 10 min, washed exhaustively with water and ethanol, and dried. Monolayers were prepared by dipping the precleaned substrates into 1 mM solutions of compounds **1**, **2**, or **3** in dichloromethane for 16 h at room temperature. The substrates were then rinsed with dichloromethane and ethanol and subsequently dried. SAMs for lattice imaging and in situ imaging of the reaction on Au(111) substrates were prepared similarly on annealed Au(111) substrates described in ref 28. These substrates consist of triangular Au(111) terraces (see below).

Instrumentation. IR spectra of monolayers were determined with a Perkin-Elmer 1725 X instrument fitted with an MCT detector and a grazing angle accessory (Spectra-Tech Inc.). Freshly cleaned (concentrated HNO_3, 10 min) bare gold slides were used as background. The sample compartment of the spectrometer was purged with nitrogen to prevent interference from water vapor. Surface plasmon resonance (SPR) data were acquired using an instrument built at the University of Sheffield, giving a resonance angle resolution of 0.006°. Thicknesses were calculated from the shift of the resonance angle using the standard Fresnel equation,[29] assuming the dielectric constant of the film to be equal to 2.1. Contact angles of water drops (1 μL) which were generated with a micrometer syringe (Agla) were recorded with a CCD camera attached to a Power Macintosh computer. Electronic images of sessile, advancing, and receding drops were stored in the computer and analyzed using ClarisDraw software. At least three drops were analyzed for each slide.

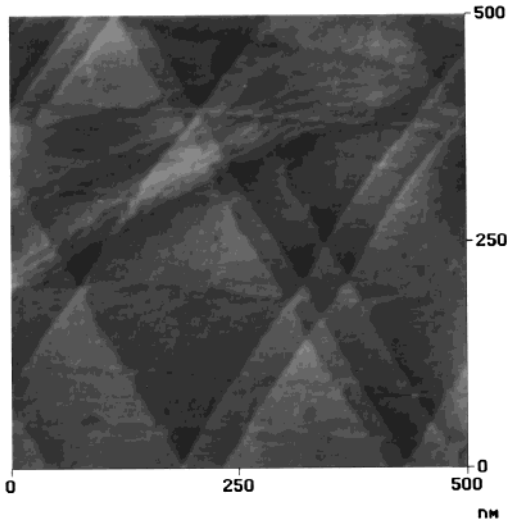

Figure 4. Tapping-mode AFM height image of Au(111) surface covered with inert octadecanethiol SAM (*z*-scale, 5.0 nm).

Table 3. Kinetics of in Situ Hydrolysis of SAMs on Gold-Covered AFM Tips

SAM	concn NaOH, (mol/L)	average half-reaction time $\tau_{1/2}$, (s)	range of induction periods, (s)
1	1.00	365	0−560
2	1.00	−	−
3	1.00	28	0
1	0.10	965	0−1100
2	0.10	630	150−435
3	0.10	220	0
1	0.01	2298	1305−1677
2	0.01	1655	100−1267
3	0.01	889	0

AFM and Tip Modification. Triangular-shaped silicon nitride cantilevers and silicon nitride tips (Digital Instruments (DI), Santa Barbara, CA) were covered with 50−70 nm of gold in a Balzers SCD 040 sputtering machine at an argon pressure of 0.1 mbar or, alternatively, with ca. 2 nm of Ti and ca. 75 nm of Au under high vacuum (Balzers). The gold-covered tips were then functionalized with SAMs of **1**, **2**, or **3** following the procedures described in refs 10b,c and 27. The AFM measurements were carried out with a NanoScope II and a NanoScope III multimode AFM (DI) using a liquid cell. Force measurements were performed with modified tips, and imaging was done with unmodified silicon nitride tips,[30] respectively. Cantilever spring constants were calibrated as described in ref 31. Tapping-mode AFM images of the Au(111) substrate were acquired as described in refs 10b,c.

Inverted CFM. The functionalized AFM tip was placed in the liquid cell. After a brief equilibration period in ultrapure water, the tip was engaged on an octadecanethiol SAM on Au(111), and a set of force−distance curves was recorded. After withdrawal of the tip, the cell was flushed with more than 20 times the cell volume of aqueous NaOH of

(27) Chechik, V.; Schönherr, H.; Vancso, G. J.; Stirling, C. J. M. *Langmuir* **1998**, *14*, 3003−3010.

(28) Schönherr, H.; Vancso, G. J.; Huisman, B.-H.; van Veggel, F. C. J. M.; Reinhoudt, D. N. *Langmuir* **1999**, *15*, 5541−5546.

(29) Hansen, W. N. *J. Opt. Soc. Am.* **1968**, *58*, 380.

(30) The tip functionalization is concomitant with an increase in tip radius. For imaging of the lattice as well as of the hydrolysis reaction of the SAMs on Au(111) substrates, the sharper unmodified tips were used.

(31) Calibration was performed using micromachined cantilevers (Park Scientific Instruments, Sunnyvale, CA) with exactly known spring constant. The procedure as well as the specifications are given in the following: Tortonese, M.; Kirk, M. *Proc. SPIE* **1997**, *3009*, 53−60. However, it should be noted that, for the evaluation of the kinetics, the absolute values of the forces are not relevant.

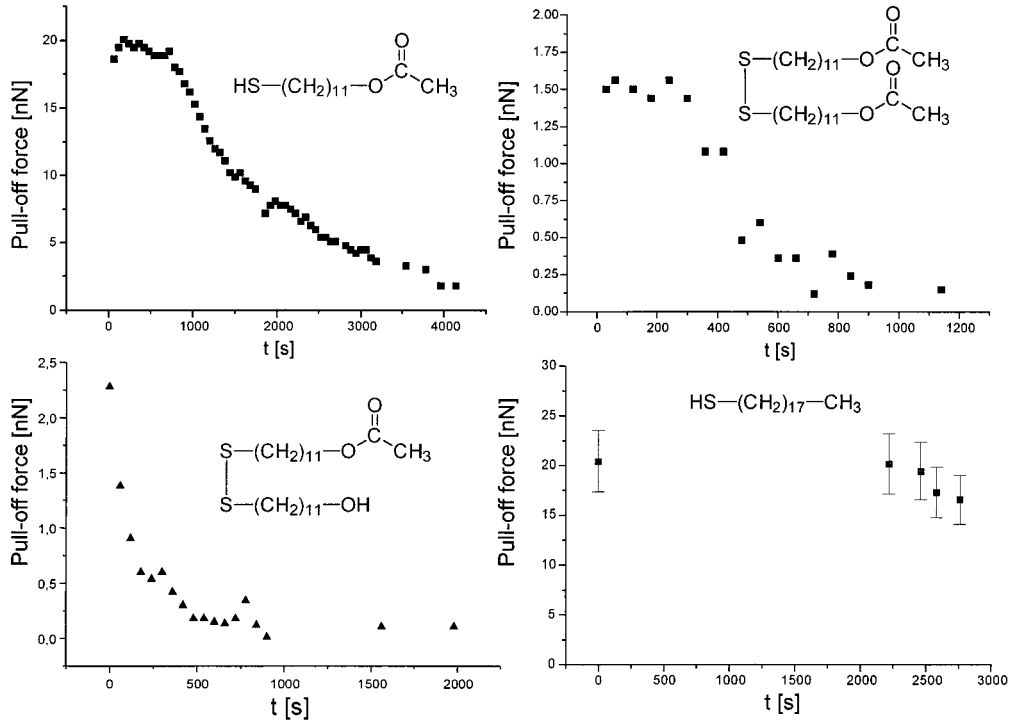

Figure 5. Pull-off forces measured during hydrolysis as a function of reaction time *t* of SAMs of **1**, **2**, **3**, and octadecanethiol (blank) in 0.1 M NaOH followed by inverted CFM. Results of representative individual experiments are shown. Note the different time scales.

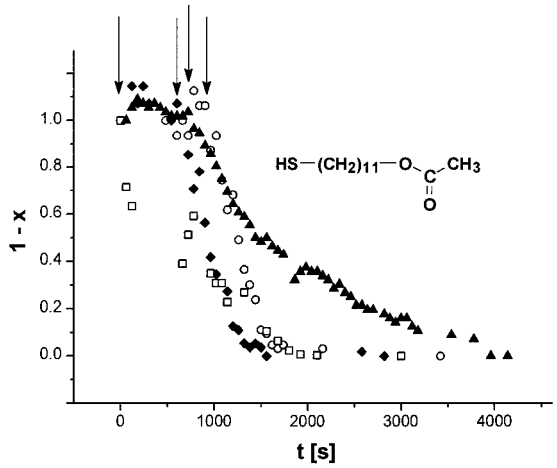

Figure 6. Hydrolysis ([1 − *x*] as a function of reaction time *t*, with extent of reaction *x*) of SAMs of **1** in 0.1 M NaOH followed by inverted CFM. Results of four individual experiments are shown. Induction periods (as indicated by arrows) vary between 0 and 1000 s. Following the induction periods, the reactions proceed at similar rates.

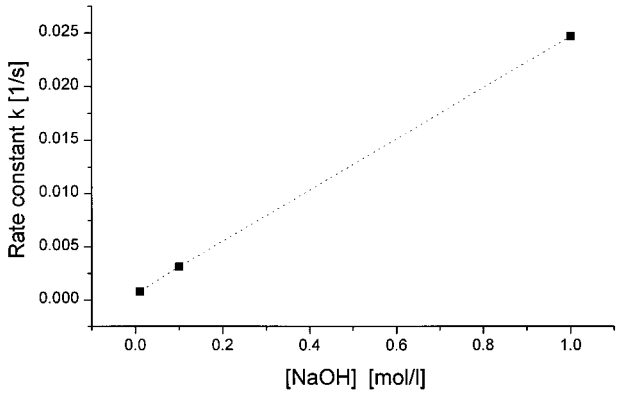

Figure 7. Pseudo-first-order rate constants for the hydrolysis reaction observed for **3** by inverted CFM, which depend linearly on the concentration of NaOH. The mean second-order rate constant k_{AFM} was 2.4×10^{-2} L mol^{-1} s^{-1}.

known concentration. When a stable photodiode reading was obtained the tip was engaged again. Immediately after engaging, force−distance curves were recorded at 30 (60)-s intervals. The mean of 10 individual pull-off events, measured after each 30 s (60 s for slow reactions), was calculated.

The conversion *x* of ester groups to hydroxyl groups was calculated from

$$x = [F_0 - F_t]/[F_0 - F_\infty] \quad (1)$$

where F_0, F_t, and F_∞ denote the measured average pull-off forces at $t = 0$, $t = t$, and $t = \infty$, respectively.[10a] This equation is based on the assumption that the forces change linearly with the work of adhesion. The surface free energy of the tip and the interfacial free energy are assumed to be influenced only by changes in the endgroup, while the surface free energy of the inert substrate is assumed to be constant.[10a]

Results and Discussion

In the following paragraphs, a number of different experiments are discussed. The structure of the SAMs of compounds **1**−**3** (Chart 1) was first investigated in detail using contact angle, FT-IR spectroscopy, and surface plasmon resonance spectroscopy. The alkaline hydrolysis of the SAMs was studied by ex situ FT-IR spectroscopy. The hydrolysis reaction was further investigated in situ by "inverted" chemical force microscopy. Finally, additional results were obtained by in situ AFM.

Self-Assembled Monolayer Structure. In this study, SAMs of the ester-terminated thiol **1**, the corresponding symmetrical disulfide **2,** and the half-ester disulfide **3** were investigated. Close packing in the monolayers of esters **1** and **2** was established by thickness (surface plasmon resonance spectroscopy) and wettability measurements (Table 1).

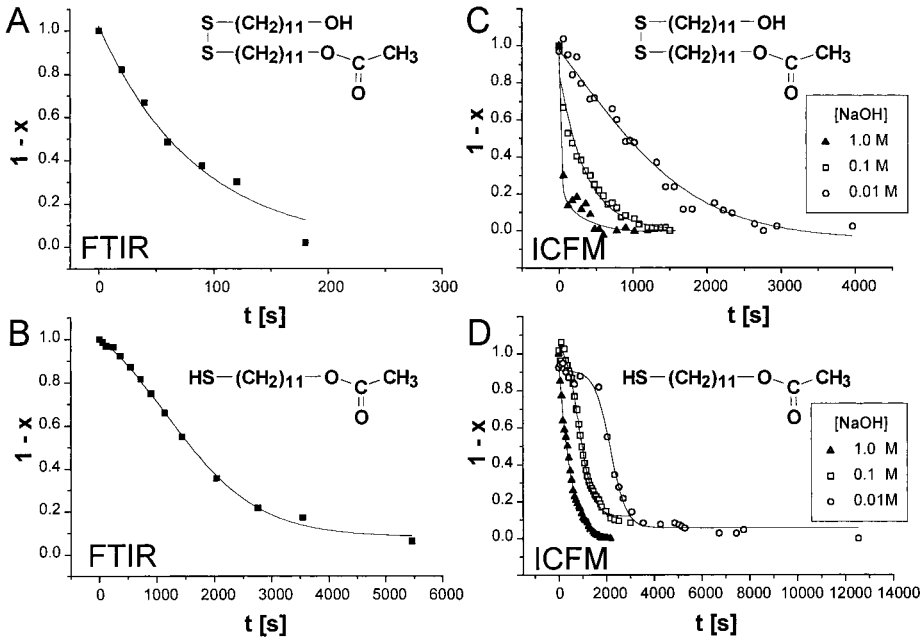

Figure 8. Course of the hydrolysis ([1 − *x*] as a function of reaction time *t*; *x* denotes the extent of the reaction) as measured by FT-IR (A,B) for 1 M NaOH and measured by inverted CFM (C,D) for various concentrations. AFM data were obtained by averaging over many individual experiments. Note the different time scales. The lines correspond to exponential or sigmoid fits; for details see text.

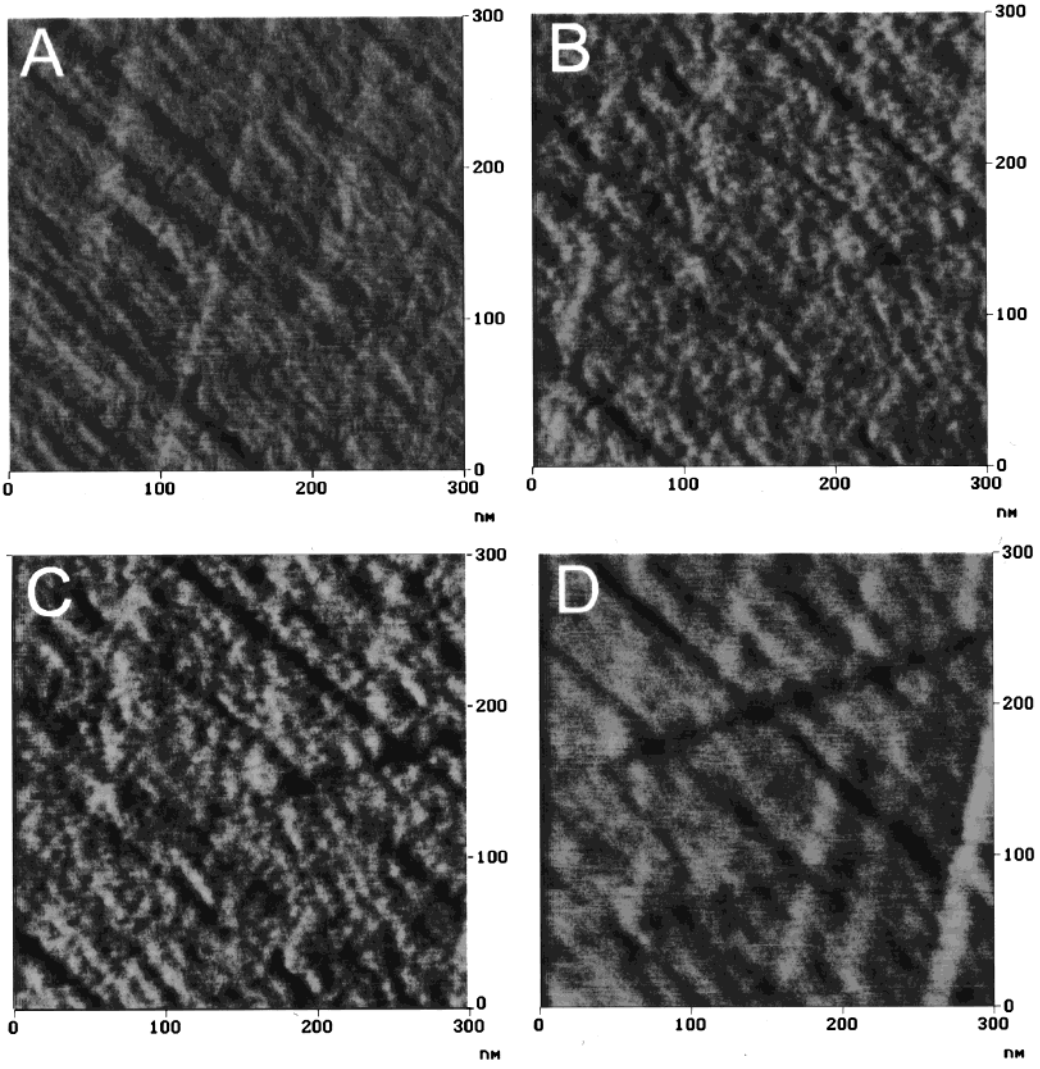

Figure 9. In situ AFM (friction mode with unmodified tip) of hydrolysis of a SAM of **1** on Au(111) in 1 M NaOH (bright color corresponds to high friction; *z*-scale from black to white, 0.05 V). The images were captured after 4 (A), 10 (B), 13 (C), and 24 min (D), respectively.

The FT-IR data were consistent with literature data on similar films.[32] The asymmetric stretching vibrations $\nu_a(CH_2)$ at 2919−2920 cm^{-1} are typical of well-packed alkane chains in an all-trans conformation.[33] The ν(C−O) vibration at 1259−1262 cm^{-1} shifted to higher frequencies as compared with bulk spectra (1240−1242 cm^{-1}), showing strong lateral interactions between adjacent carbonyl groups in ordered quasi-crystalline environments.[34] SAMs of **3** showed a higher frequency $\nu_a(CH_2)$ vibration (2922 cm^{-1}), and the water contact angle of SAMs of **3** was lower than those of **1** and **2**, indicating partial exposure of hydroxyl groups at the monolayer surface.[35] Molecular (lattice) resolution AFM measurements performed in water revealed a hexagonal tail group lattice structure with a lattice constant of 5.2 ± 0.2 Å (vide infra).[16] Monolayers of **1**, **2**, and **3** thus possess a well-packed structure. AFM friction force measurements (vide infra) were consistent with the interpretation that the hydroxyl and ester groups in the monolayer of **3** are evenly distributed down to the level of the lateral size range of the contact area between AFM tip and sample surface.[36]

Ester Hydrolysis Studied ex Situ by FT-IR. All reactions were carried out in 1.0 M aqueous sodium hydroxide at room temperature. Macroscopic kinetics were determined by FT-IR spectroscopy by following the decrease of the integrated intensity of the ν(C═O), ν(C−O), and $\delta_s(CH_3)$ vibrations ex situ. SAMs of thiol **1** (and disulfide **2**) reacted much more slowly than SAMs of the mixed disulfide **3** (Figure 2). Kinetics of the mixed disulfide **3** were exponential, while **1** and **2** showed sigmoid behavior. The half-reaction times are listed in Table 2. For the mixed disulfide **3**, the pseudo-first-order rate constant k_{FT-IR} was 1.00×10^{-2} s^{-1}.

In monolayers **1** and **2**, which present a close-packed surface, access of hydroxide ions to the carboxyl groups appears to be hindered even though the reactive carboxyl groups are buried only a few angstroms below the surface. Similar sigmoid kinetics are found, for example, in surface reactions of perfect crystals which often exhibit low initial reactivity.[37] In these cases, defects at the crystal surface may allow a slow initial reaction, and acceleration is observed as more reactive sites become exposed.[38] SAMs of esters **1** and **2**, at half-hydrolysis (i.e., with 50% of the ester groups transformed into hydroxyl groups), would at first sight appear structurally equivalent to the mixed disulfide **3**. Reaction of esters **1** and **2** at 50% conversion is, however, ca.10−20 times slower than that of ester **3**.[39]

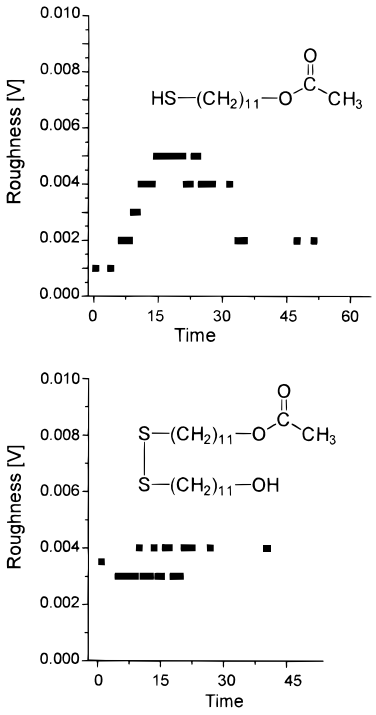

Figure 10. Roughness analysis of friction images (such as those shown in Figure 9) of SAM of **1** (top) and disulfide **3** (bottom) for hydrolysis in 1 M NaOH.

Ester Hydrolysis Studied in Situ by Inverted CFM. The origin of the striking reactivity difference mentioned at the end of the previous paragraph must lie in the intimate structure of the surface of the SAMs. Thus, it is of interest to obtain structural and compositional information with high resolution, preferably on the molecular scale. In situ information on the composition of the reacting monolayers was obtained by the ICFM approach described above. In these experiments, the force required to pull the AFM tip coated with **1**, **2**, or **3** away from contact with an inert octadecanethiol SAM on flat Au(111) was followed in real time in situ during the hydrolysis.

The change in surface composition could be measured accurately because the hydrophobic force between ester (the reactant)- and alkyl-terminated surfaces is large. Average pull-off forces measured between *neat* ester-terminated SAMs and methyl-terminated tips were found to be 9 ± 2 nN, whereas neat hydroxyl-terminated SAMs and methyl-terminated tips show an average pull-off force of 0.4 ± 0.3 nN (Figure 3). These forces follow the trends which were previously observed and explained by the Johnson-Kendall−Roberts theory of contact mechanics.[17,40]

As the contact sampling area of the functionalized AFM tip is between 10 and 100 molecules, depending on the actual tip radius,[17] the reaction can be studied in a highly localized fashion. The Au(111) substrates are atomically smooth over distances of several hundred nanometers, with only occasional steps and depressions present (Figure 4). With highly ordered octadecanethiol SAMs on top of these substrates, interaction between exactly the same functional groups at the tip apex and a homogeneous inert substrate is ensured.

The *individual* reaction profiles for thiol **1** and disulfide **2** showed significant induction periods which depend on the hydroxide concentration (Figure 5, Table 3). This is indicative of an activated process of nucleation and growth. For SAMs of

(32) (a) Nuzzo, R. G.; Dubois, L. H.; Allara, D. L. *J. Am. Chem. Soc.* **1990**, *112*, 558−569. (b) Engquist, I.; Lestelius, M.; Liedberg, B. *Langmuir* **1997**, *13*, 4003−4012.

(33) Porter, M. D.; Bright, T. B.; Allara, D. L.; Chidsey, C. E. D. *J. Am. Chem. Soc.* **1987**, *109*, 3559−3568.

(34) Sondag, A. H. M.; Tol, A. J. W.; Touwslager, F. J. *Langmuir* **1992**, *8*, 1127−1135.

(35) Takami, T.; Delamarche, E.; Michel, B.; Gerber, Ch.; Wolf, H.; Ringsdorf, H. *Langmuir* **1995**, *11*, 3876−3881.

(36) There is ample evidence that mixed disulfides do not phase-separate at room temperature. (a) Reference 35. (b) Schönherr, H.; Ringsdorf, H.; Jaschke, M.; Butt, H.-J.; Bamberg, E.; Allinson, H.; Evans, S. D. *Langmuir* **1996**, *12*, 3898−3904. (c) Tsao, M.-W.; Rabolt, J. F.; Schönherr, H.; Castner, D. *Langmuir* **2000**, *16*, 1734−1743.

(37) Harrison, L. G. In *Comprehensive Chemical Kinetics, Vol. 2, The Theory of Kinetics*; Bamford, C. H., Tipper, C. F. H., Eds.; Elsevier: Amsterdam, 1969; pp 377−462.

(38) A recent study showed that imaging the monolayer of a succinimide ester with AFM disrupts the order strongly enough to appreciably accelerate hydrolysis (Wang, J.; Kenseth, J. R.; Jones, V. W.; Green, J.-B. D.; McDermott, M. T.; Porter, M. D. *J. Am. Chem. Soc.* **1997**, *119*, 12796−12799).

(39) Intramolecular general base catalysis [which could be responsible for the autocatalytic (sigmoid) behavior] can be excluded on the basis of control experiments with mixed disulfides in which one chain carries a terminal ester group and the other a terminal methyl group (Chechik, V.; Stirling, C. J. M., unpublished work).

(40) Johnson, K. L.; Kendall, K.; Roberts, A. D. *Proc. R. Soc. London A* **1971**, *324*, 301−313.

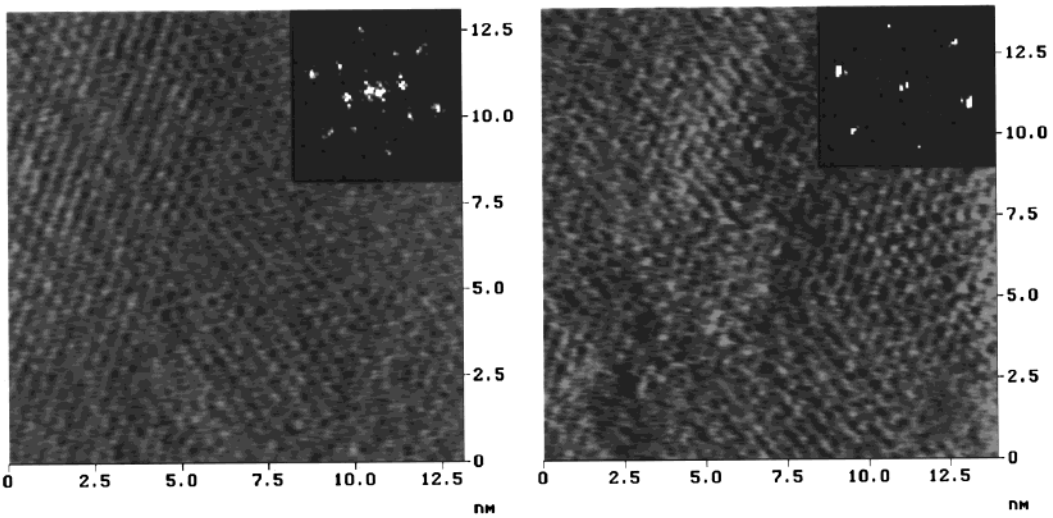

Figure 11. Unprocessed AFM images of SAM of **1** prior to (left) and after (right) hydrolysis in 1 M NaOH (inset, 2-D fast Fourier transform).

the mixed disulfide **3**, no induction periods were observed. Test experiments with (inert) octadecanethiol-coated tips showed that SAM damage can be excluded and that the SAM/gold assembly stays intact over the typical experiment times. The AFM results are summarized in Table 3.

In Figure 6, the results of four different experiments for thiol **1** performed under identical conditions are shown. The *individual* reaction profiles showed a wide distribution of induction periods, indicated by the arrows.

The contact area between the tip and the surface at pull-off is smaller than the typical domain size in SAMs.[41] If the reaction starts at defect sites, variable induction periods are to be attributed to the time elapsed before a defect is formed in the contact area between ester-modified tip and alkyl-terminated inert surface. If a defect is already present in the contact area, the reaction is being observed immediately after engagement, and the induction period is small or nonexistent. If there are no defects in the contact area, the reaction is not observed until a defect is formed, or the reaction front reaches the contact area. This interpretation is in good agreement with an estimate of the domain size based on the observed induction times and reaction kinetics.[42] From the data summarized in Table 3, a maximum domain size of 3.2 ± 0.2 nm for thiol **1**, and 2.6 ± 1.2 nm for the symmetric disulfide **2**, can be estimated.[42] These values are in agreement with literature data.[43]

It can be concluded at this point that the observed distribution of induction periods is a strong indication of separation of reacted ($-$OH) and unreacted ($-$O$-$CO$-$CH$_3$) terminal groups during the hydrolysis. Thus, the profiles of the different experiments shown in Figure 6 differ because ICFM follows the reaction with very high lateral resolution.

The kinetic profiles in the continuum limit were estimated by averaging many AFM experiments. These profiles were found to be very similar to the FT-IR profiles. The reaction of SAMs of half-ester disulfide **3** (Figure 8C) gives an *average* second-order rate constant $k_{AFM} = 2.4 \times 10^{-2}$ L mol^{-1} s^{-1}, which is in good agreement with the value obtained by FT-IR (Figures 7 and 8).[44] By contrast, the SAMs of both thiol **1** and symmetrical disulfide **2** showed sigmoid profiles for the average kinetics (Figure 8). Macroscale kinetics determined by FT-IR can thus be reproduced by averaging snapshots of the reaction of 10$-$100 molecules from the AFM experiments.

In Situ AFM Imaging of SAMs during Hydrolysis. Further indication for the formation of domains of reacted and unreacted molecules during the hydrolysis reaction is obtained from in situ contact mode AFM experiments with uncoated tips on SAMs of **1** and **3** on flat Au(111) substrates. As shown in Figure 9, the friction force observed on Au(111) terraces covered with a SAM of **1** changes significantly during hydrolysis. After ca. 4 min, the smooth image which shows only the step edges of the Au surface began to change to an image exhibiting a "rippled" appearance. The inhomogeneous friction producing the ripples increased and then disappeared during the course of the reaction. We postulate that the observed "ripples" are related to inhomogeneous adhesion, and hence friction,[17,20] because of the formation of domains of reacted and unreacted molecules during the course of the reaction.[45]

The inhomogeneous friction producing the ripples can be evaluated by analyzing the deviation of the friction for each pixel from the mean value similar to a roughness analysis.[46] The corresponding roughness data as a function of reaction time

(41) Typical domain sizes of SAMs on gold which has not been heat-treated after assembly are in the order of 5 nm (Delamarche, E.; Michel, B.; Gerber, Ch.; Anselmetti, D.; Güntherodt, H.-J.; Wolf, H.; Ringsdorf, H. *Langmuir* **1994**, *10*, 2869$-$2871).

(42) For this rough estimate, a circular domain shape was assumed. The longest induction period was assigned to the idealized situation in which the circular contact area (with radius r_o) is centered on this domain. As there are no defects in the contact area, the reaction is not observed until the reaction front, which starts at the domain boundary, reaches the contact area. On the basis of Johnson$-$Kendall$-$Roberts theory, the original contact area was calculated ($K = 4.7 \times 10^{10}$ Pa; $W_{12}(t = 0) = 50$ mN/m). A reaction rate was defined as the ratio of r_o and reaction time t_R (t_R is the time elapsed between the first decrease in adhesion forces and the end of changes). Using this rate (in nm/s), the original domain size can be calculated on the basis of the observed induction time.

(43) It is reasonable to assume that the domain sizes on sputtered or evaporated gold are smaller than that on flat Au(111). Experimental evidence for small crystalline patches further supports this assumption, see: Schönherr, H.; Vancso, G. J. *Langmuir* **1997**, *13*, 3769$-$3774.

(44) Quantitative differences between the AFM and FT-IR results can be explained by the fact that the sampling area for AFM is more than ca. 10^{12} times smaller than for FT-IR and that reactions, e.g., at grain boundaries would not affect the AFM results.

(45) The true resolution of the AFM is not sufficiently high to unequivocally enable one to image subdomain details. In addition, it is not a priori clear how the friction measured on a few molecules can be related to exposed functional groups.

(46) The mean roughness R_A of a surface is defined as the standard deviation of the height with respect to the center plane within the scan area selected. The R_A values were obtained according to the following equation: $R_A = (\sum_{x=1,N;y=1,M}(z_{xy} - \bar{z}_{xy})^2/[(N-1)(M-1)])^{1/2}$, where N and M are the numbers of pixels in the x and y directions, respectively, and $z_{x,y}$ is the image pixel height with respect to the center plane height $\bar{z}_{xy}$ for the pixel (x,y).

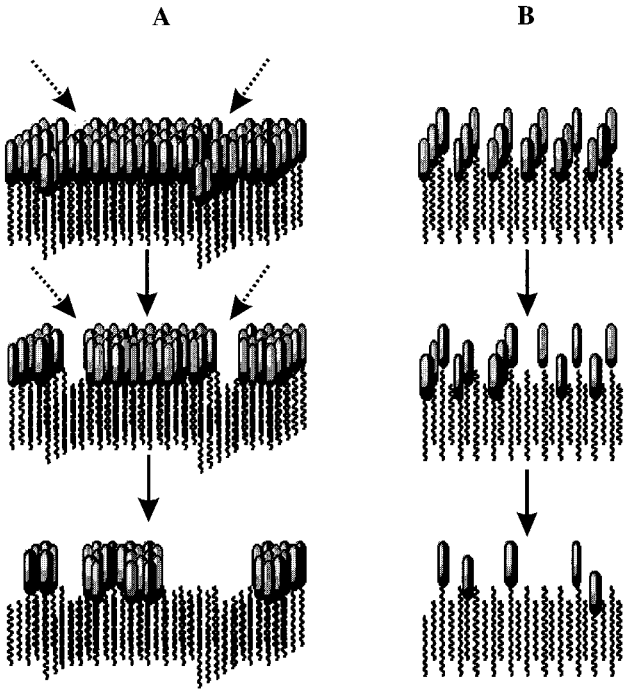

Figure 12. Schematic representation of (A) inhomogeneous reactions for SAMs of thiol **1** and disulfide **2** and (B) the homogeneous reaction of mixed disulfide **3**. The reaction of **1** starts at defect sites (indicated by arrows) and creates domains of reacted and unreacted molecules. The reaction then proceeds at these domain boundaries until all molecules have reacted, while for **3** the reaction occurs homogeneously.

are shown in Figure 10. The friction contrast peaks after ca. 15 min for thiol **1**, while there is no contrast change for mixed disulfide **3**. These observations are in agreement with the FT-IR and ICFM results.

The lattice of the SAMs could be imaged with molecular (lattice) resolution prior to and after the hydrolysis on the Au(111) terraces shown in Figure 9. In Figure 11, the corresponding high-resolution lattice images are displayed. The fact that lattice imaging was possible prior to and after the hydrolysis demonstrates that SAM damage can be excluded as a basis for the disappearing inhomogeneity of the friction images of **1**. The true resolution of the friction measurements can be assumed to be in the order of 2−5 nm, which is a typical size for domains in SAMs.[41,45] As the friction contrast did not change significantly in SAMs of the mixed disulfide **3**, the inhomogeneous friction observed for thiol **1** strongly suggests that the reaction proceeds inhomogeneously for SAMs of **1**.

The scenario proposed for the reaction in well-packed SAMs is depicted schematically in Figure 12. The mechanism shown is consistent with the AFM and FT-IR data and accounts for the reactivity differences between half-reacted monolayers of **1** and **2** on one hand and the monolayers of **3** on the other. While the layer of **3** remains topographically homogeneous, **1** and **2** separate into domains during the hydrolysis.

Conclusions

We have demonstrated for the first time that average macroscopic kinetics of reactions in SAMs can be correlated and explained by nanometer-level force (adhesion) measurements in the confined environment of the monolayer studied. Using a modified CFM approach, which we termed "inverted chemical force microscopy", reactions of as few as 10−100 molecules could be followed in situ. Structure−reactivity differences, arising from differences in monolayer structure, as observed on the nanometer scale, on average agree well with macroscopic behavior observed by FT-IR. The studies show that reagents penetrate functionalized monolayers at specific defect sites or at domain boundaries.

Acknowledgment. This research was financially supported by the Council for Chemical Sciences of The Netherlands Organization for Scientific Research (CW-NWO) in the priority program materials (PPM), by the Engineering and Physical Sciences Research Council of the U.K., and by the University of Sheffield.

JA9902569